Sustainable and Clean Buildings
https://ojs.wiserpub.com/index.php/SCB/

UNIVERSAL WISER PUBLISHER

Research Article

A Novel Moist Airflow Heating System for Low/Zero Carbon Buildings: a Numerical Study

Pinar Mert Cuce[1,2,3*], **Saffa Riffat**[4]

[1]Department of Architecture, Faculty of Engineering and Architecture, Recep Tayyip Erdogan University, Zihni Derin Campus, 53100, Rize, Turkey
[2]Department of Energy Systems Engineering, Faculty of Engineering and Architecture, Recep Tayyip Erdogan University, Zihni Derin Campus, 53100, Rize, Turkey
[3]College of Built Environment, Birmingham City University, Birmingham, United Kingdom
[4]Department of Architecture and Built Environment, University of Nottingham, Nottingham, NG7 2RD, United Kingdom
E-mail: pinar.mertcuce@erdogan.edu.tr

Received: 2 March 2024; **Revised:** 18 May 2024; **Accepted:** 27 May 2024

Abstract: As people spend a significant portion of their day indoors, ensuring comfortable interior environments has become an unavoidable reality. Heating assumes paramount significance in regions characterised by prolonged exposure to cold climates, notably in European countries. However, the traditional heating systems currently employed for indoor heating often contribute to adverse environmental effects. This study introduces a newly devised passive heating system aimed at mitigating or potentially replacing prevailing traditional heating methods. This proposed system is theoretically researched and interpreted by integrating it within a building. Three different drive fluids (water, moist air, and air) are considered, with each fluid's components analysed separately in accordance with the thermodynamic principles. Through these assessments, the proposed system emerges as environmentally sustainable and highly adaptable to contemporary building contexts. Furthermore, its cost-effectiveness surpasses that of conventional heating systems, marking a significant advancement in heating technology. While the coefficient of performance (COP) of the proposed system stands at approximately 1.307 when powered by electrical energy, it can surge up to 13.878 when powered by renewable energy systems such as solar collector and photovoltaic (PV).

***Keywords*:** heating, ventilation, and air conditioning (HVAC) systems, low-cost heating, buildings, energy efficiency, renewable energy systems

Nomenclature

$\dot{E}$	energy (W)
Q	heat transfer rate (W)
h	heat transfer coefficient (W/m^2·K)
T	temperature (°C)
A	surface area (m^2)
c	specific heat capacity (kJ/kg·K)
$\dot{m}$	mass flow rate (kg/s)

DOI:

k	thermal conductivity (W/m·K)
n	constant
H	enthalpy (kJ/kg)
P	power (W)
L	length of channel (m)
v	velocity (m/s)
D	channel diameter (m)
G	intensity of the sun (W/m^2)
t	time (s)
Nu	nusselt number
Re	reynolds number
Pr	prandtl number (m^2/s)
MAS	moist airflow system
COP	coefficient of performance

Subscripts

in	input
sc	solar collector
avg	average
df	drive fluid
$evap$	evaporative
fs	first state
he	heat exchange
ps	proposed system
out	output
es	energy stored
ma	moist air
dc	duct
ea	energy absorbed
ls	latest state
tec	thermal energy content
hyd	hydraulic

Greek symbols

ρ	density (m^3/kg)
ω	humidity ratio ($g_{wet\ air}/kg_{air}$)
u	dynamic viscosity (kg/m·s)
α	absorption coefficient

1. Introduction

Buildings represent one of the most crucial sectors in global energy consumption, playing a pivotal role in utilising critical energy resources worldwide [1]. In recent times, the rise in urbanisation and industrialisation is heightened the demand for the construction sector [2]. It is widely acknowledged that it encompasses about 30% of the global greenhouse gas emissions emitted from buildings [3] and constitutes there about 40% of the worldwide energy consumed within buildings [4-5]. Within Europe, it comprises 36% of the greenhouse gas emissions emitted

by buildings [6] and encompasses 40% of the energy consumed by buildings [7-8]. Heating, ventilation, and air conditioning (HVAC) systems included up to approximately 40% of the aggregate energy consumption in buildings [9]. Traditional heating systems are commonly employed as the primary heating method within HVAC systems [10]. Regrettably, conventional heating methods frequently result in significant environmental harm, with the CO_2 they emit playing a pivotal role in such damage [11-12]. Moreover, the first installation expenses and immediate electricity usage associated with traditional heating systems are notably steep [13]. Consequently, when taking this information into account, forecasts indicate that the escalating urbanisation stemming from population growth will heighten global energy requirements and greenhouse gas emissions [14]. Within this framework, the existence of buildings within the global energy context assumes significant importance owing to the prevalence of inefficient technologies in building infrastructure [15-16]. The air tightness of buildings assumes heightened importance owing to its profound impacts on both energy consumption and indoor air qualification [17]. With the rising demand for comfort driven by the expanding human population and technological advancements, the heating requirements of buildings are on the rise [18]. Through conducted studies and the development of new systems, studies have managed to curtail or stabilise the energy needed for residential heating [19-20]. Certainly, research on this subject, particularly investigations into passive heating techniques, remains the primary focus of attention and continues to evolve [21-22]. Conventional heating systems in buildings typically rely on heating a drive fluid, predominantly water. This system also boasts a complex structure, and the fluid it contains drives up costs due to its notably high specific heat capacity. Furthermore, the pumping systems within these traditional setups entail considerable maintenance expenses [23]. Hence, the choice of the drive fluid is crucial, as it can substantially influence the cost-effective implementation of heating demands in buildings. Air stands out for its significantly lower specific heat capacity compared to other drive fluids [24-25]. This characteristic allows air to achieve high-temperature differences with minimal energy input [26]. When contemplating building design, durability and aesthetics take centre stage [27]. Hence, when incorporating an innovative system into a building, it is imperative to elaborate on more than just its cost-effectiveness, environmental benefits, and novelty. It is equally essential to consider its spatial requirements within the building, its visual impact, and potential future drawbacks [28-30]. This study introduces an innovative air-based heating system, capitalising on air's inherent properties, in conjunction with optimal building design. Unlike traditional heating systems, this recommended heating system is touted for its environmentally friendly and cost-effective features. Both numerically and theoretically, the seamless integrability of this newly proposed heating system into contemporary buildings is demonstrated in this study. This article aims to serve as a wellspring of inspiration for the future development of heating systems tailored specifically for Low/Zero energy buildings. In future endeavours, MAS will be integrated into a building, undergoing experimental testing. All theoretical conditions and numerical analyses outlined in the article will be comprehensively evaluated in this integrated system.

2. Moist airflow system

The moist airflow system (MAS) represents a cost-effective heating solution that primarily utilises air as it is fluid medium. The waste heat generated by factories serves as the primary power source for MAS. The energy derived from this source is primarily aimed at effectively reducing the heating energy needed to warm buildings. In addition to waste heat, the system can also be implemented within buildings that are equipped with renewable energy technologies, such as solar water-air collectors, as shown in Figure 1.

The innovative and straightforward applicability of MAS lies in its use of air rather than water as the drive fluid. Consequently, heat energy can be transferred to the air for heating a space, utilising the heat energy stored in water sourced from waste heat or renewable energy sources. When MAS is fuelled by solar energy, water is extracted from the source and conducted to the solar collectors for utilisation. Water carrying heightened heat energy (within the laws of thermodynamics, it is assumed that there are no losses) is stored in an insulated water storage tank without any loss of energy. The temperature of water housed in the insulated water tank ranges between 30-90 °C. By leveraging the control unit, the temperature of the water can be adjusted based on the available solar energy. Therefore, in the natural evaporation process, warm and moist air accumulates at the top of the tank, serving as the source for space heating. Warm and moist air is conveyed to the indoor space through insulated pipes to effectively distribute air enriched with heat energy to the colder environment. During this heating process, it is assumed that the moist air remains in

adiabatic satiation. As moist air traverses the cold surroundings, it gradually loses its heat energy content and undergoes condensation. Condensed water from moist air is gathered and stored in a specific condensation tank, as depicted in Figure 1. Subsequently, the condensed water stored in the condensation tank is pumped to the storage tank. This cycle persists as energy continues to be derived from renewable sources. Furthermore, the operational principle of the MAS is depicted in Figure 2.

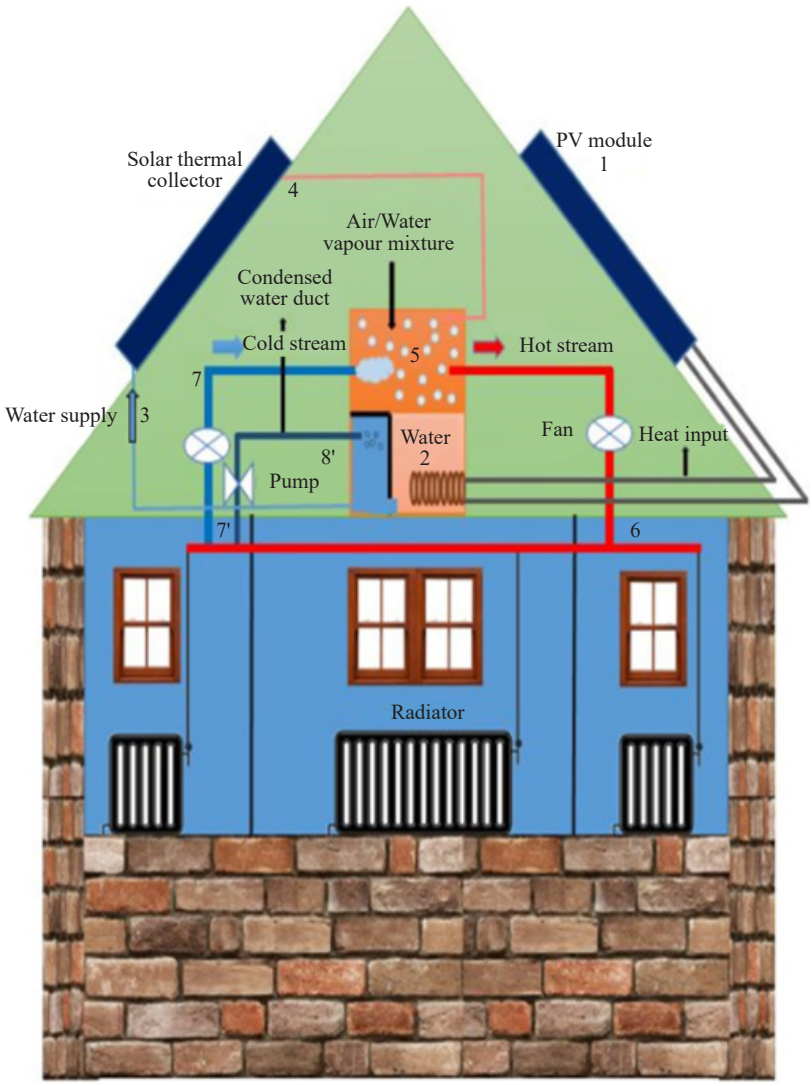

1-2: Pre-heating the process water using a PV module before it enters the solar collector.
2-3: The delivery of pre-heated process water to the solar collector.
3-4: Heating the process water as it passes through the solar collector and changes from to warm air.
4-5: Routing the heated water-steam mixture to the chamber.
5-6: Guiding the hot water-steam mixture towards the honeycombs for room heating.
6-7: Merging the spent mixture with the heated water-steam blend for recycling.
6-7'-8': Channelling surplus water from the mixture to the reservoir for eventual return to the collector.

Figure 1. Illustration of the proposed MAS

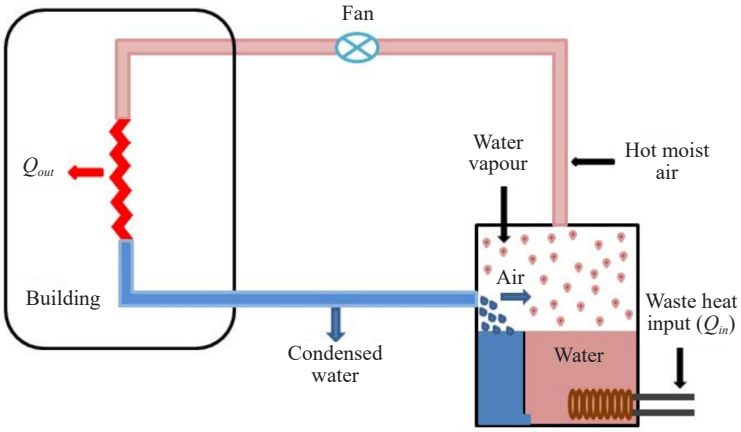

Figure 2. Working principle of the MAS

3. Thermodynamic model of moist airflow system

This section delves into the MAS within the realm of thermodynamic laws. The first law of thermodynamics is employed to analyse each component of the system independently. In adherence to the law of energy conservation, the system meticulously establishes an energy balance for both air and water components. Considering the adiabatic boundary provisos across the system, the heat energy stored in water is expressed as follows:

$$\dot{E}_{in,\,sc} = \dot{E}_{out,\,es} \tag{1}$$

The incoming *sc* is represented as:

$$\dot{E}_{in,\,sc} = \alpha \cdot G \cdot A_{sc} \tag{2}$$

The heat energy stored in water results in a temperature rise, resulting in the storage of sensible heat energy, the process is described as follows:

$$\dot{E}_{out,\,es} = m_{water} \cdot c_{water} \cdot \Delta T_{fs\ and\ ls} \tag{3}$$

The stored heat energy in the water accelerates evaporation within the water tank, leading to the formation of hot and humid air at the top of the tank, as illustrated in Figure 3.

$$\Delta H_{evap} = H_{vapour} - H_{liquid} \tag{4}$$

The enthalpy of vaporisation varies with temperature, making it a temperature-dependent function. As the evaporation process proceeds, it eventually reaches the adiabatic saturation condition. This condition is characterised by the intersection of dry and wet bulb temperatures on the psychrometric diagram. The high-temperature saturated air is diverted towards the chill ambience to distribute its energy content, and the resulting enthalpy change associated with the energy change of the working air is expressed as follows:

$$E_{tec} = H_{air|fs} - H_{air|ls} \tag{5}$$

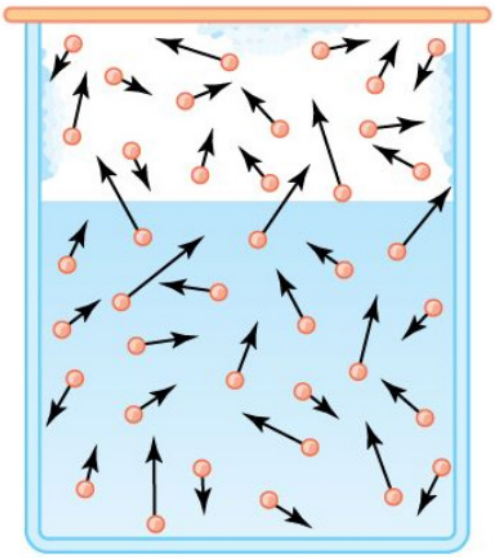

Figure 3. The evaporation and generation of moist air within the water tank

The energy exchange mentioned in this context is illustrated in Figure 4.

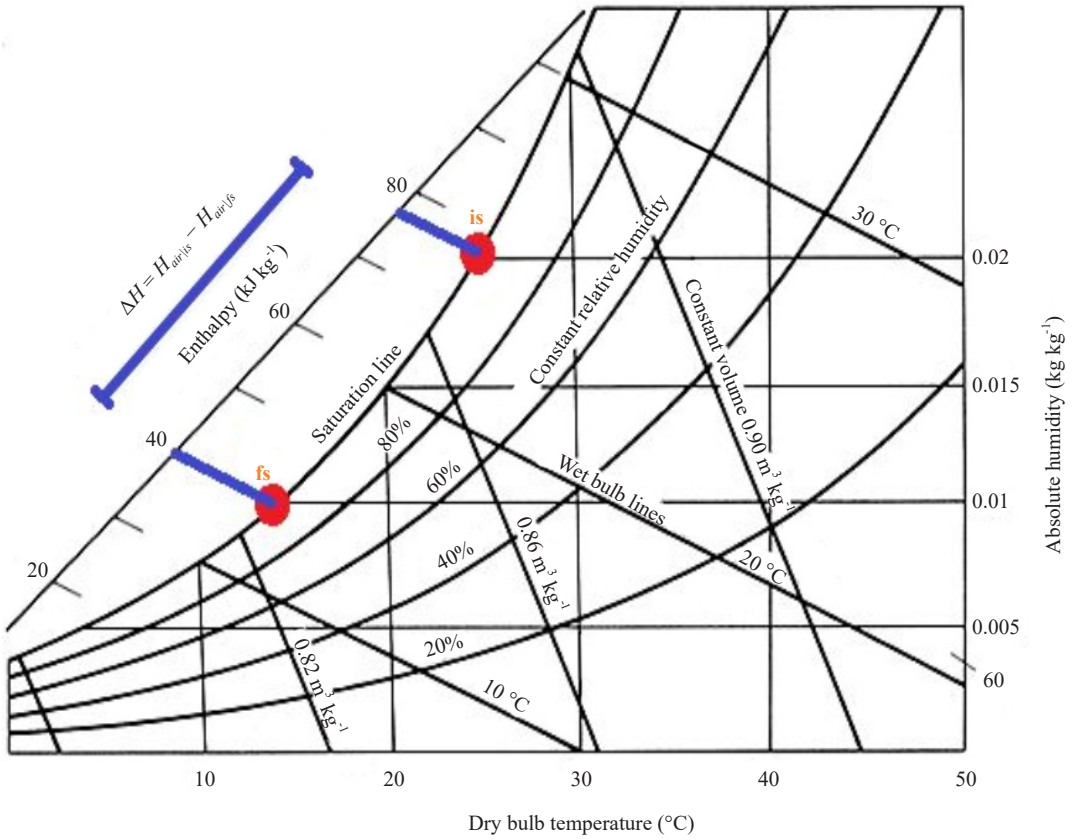

Figure 4. Enthalpy exchange of WA in psychrometric chart

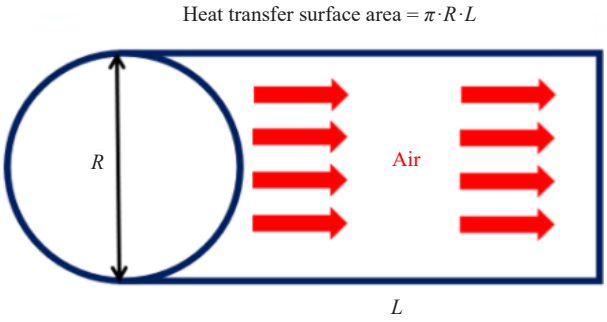

Figure 5. Surface area for heat transfer in annular tube

4. Heat transfer analysis of moist airflow system

A circular pipe efficiently transfers heat within the MAS while minimising pressure loss. The determination of the channel diameter in the system is carried out through specific methods. Additionally, the flow pattern within the channel is established by analysing the Reynolds number (*Re*) [31]. Given that the *Re* calculated within the system surpasses 2,500, it is acknowledged that the flow pattern within the channel exhibits turbulent flow. The *Re* is expressed as:

$$Re = \frac{v_{air} \cdot D_{hyd}}{u_{air}} \tag{6}$$

The following equation can express the Nusselt number (*Nu*):

$$Nu = \frac{h \cdot D_h}{k} \tag{7}$$

In practical applications where pipes typically have L/D $\gg$ 10, turbulent flows are generally considered fully developed [32]. Consequently, the Nu might be clarified using the Dittus-Boelter Correlation as:

$$Nu = 0.023 \cdot Re^{0.8} \cdot Pr^{n} \tag{8}$$

In this context, the parameter '*n*' assumes values of 0.4 for rise to heat on fluid and 0.3 for chilling it.

According to Newton's law of cooling, the mathematical expression governing the proportion of heat transfer to or from a fluid flowing in an annular tube may be elucidated:

$$Q = h \cdot A \cdot \Delta T \tag{9}$$

The mean air temperature is decisive by taking the mean of the inlet and outlet temperatures of the air, as depicted in the equation below:

$$T_{avg} = \frac{T_{in,\,air} + T_{out,\,air}}{2} \tag{10}$$

The determination of the power output of the MAS hinges on the specific temperature change within the system. The power output of the MAS can be explained at given a specific temperature as follows:

$$P_{out,\,ps} = \frac{\Delta H}{t_{he}} \tag{11}$$

The surface area for heat transfer of the MAS for an annular pipe is illustrated in Figure 5.

5. Duct diameter analysis

An analysis of the diameter of the duct is conducted for air, humid air, and water-based heating systems, considering constant energy inlet and length of duct per meter. This analysis adheres to the principle of energy conservation applied to inner flow heat transfer problems. A consistent 1 kW heat input is used in the system, providing a benchmark for performance optimisation. Moreover, the heat inlet can be adjusted appertain on request, considering factors such as temperature difference. To ensure independence from changes in other parameters, the channel diameter analysis is conducted per meter length of the channel. Following the first law of thermodynamics, the energy balance for the system is established as follows:

$$\dot{E}_{in,\,ps} = \dot{E}_{out,\,ps} \tag{12}$$

$\dot{E}_{out,\,ps}$ represents the energy absorbed by the working, corresponding to the temperature increase of the drive fluid:

$$\dot{E}_{out,\ ps} = \dot{m}_{df} \cdot c_{df} \cdot \Delta T \tag{13}$$

$\dot{E}_{out,\,ps}$ corresponds to the enthalpy change in the first and latest states of the drive fluid:

$$\dot{E}_{out,\ ps} = \dot{m}_{df} \cdot \Delta H \tag{14}$$

The $\dot{m}_{df}$ a pivotal factor influencing the parameters received and provided by the drive fluid, is expressed as follows:

$$\dot{m}_{df} = \rho_{df} \cdot v_{df} \cdot A_{ch} \tag{15}$$

Additionally, A_{ch} denotes the cross-sectional area of the channel, calculated as follows:

$$A_{ch} = \pi \frac{D^2}{4} \tag{16}$$

Notably, in the drive fluid, the specific heat capacity and density are temperature-addicted characteristics. To ensure the reliability of a calculation, it is essential to consider these characteristics at an average temperature.

$$T_{avg} = \frac{T_{df,\,in} + T_{df,\,out}}{2} \tag{17}$$

Considering Equations (13)-(17), $\dot{E}_{out,\,ps}$ can be expressed generally as follows:

$$\dot{E}_{out,\ ps} = \rho_{df} \cdot v_{df} \cdot c_{df} \cdot \Delta T_{df} \cdot \pi \cdot \frac{D^2}{4} \tag{18}$$

In this context, the determination of the channel diameter is based on the unit channel length and varies depending on the chosen drive fluid options, including air, moist air, and water. The obtained results are then compared across different temperature differences at the inlet and outlet of the drive fluid.

The determination of the specific heat capacity must consider the humidity level across the humid air diameter of the duct. Hence, the moist air specific heat at an average temperature is determined as follows:

$$c_{ma} = 1.005 + 1.82\omega_{ma} \tag{18}$$

To ensure reliable analyses, a recommended fluid speed of 0.5 m/s is assumed.

6. Results and discussion

Under this section, critical results concerning the thermodynamic optimisation, heat transfer analysis, and diameter of the duct analysis of MAS are provided, each discussed under separate subheadings. This organisational approach enables a comprehensive evaluation of each parameter.

6.1 *Thermodynamic optimisation of moist airflow system*

The numerical analysis of MAS involved specific assumptions regarding the water and air is operated within the system. Primarily, the heat energy entrance to water per unit mass of water is considered. The first water temperature is putative to be 15 °C, reflecting the mean water temperature from the network. The latest state of water temperature is treated as an unattached parameter, varying between 30-90 °C depending on the provided solar energy, as outlined in Table 1. The variation in energy required per unit mass of water corresponding to the desired water temperature is depicted in Figure 6 (a). Determining the energy required to achieve fully saturated moist air involves incorporating the enthalpy of evaporation of water into the waste heat, as detailed in Table 1. The energy requirement for the operation air in the MAS is illustrated in Figure 6 (b). This figure provides insights into the energy dynamics and demands within the MAS, crucial for understanding its operational characteristics and optimising its performance.

Table 1. The first and latest water temperatures were considered for the MAS

First water temperature (°C)	Latest water temperature (°C)	Mass of water (kg)	Waste heat required (kJ)
15	30	1	62.7
15	35	1	83.6
15	40	1	104.5
15	45	1	125.4
15	50	1	146.3
15	55	1	167.2
15	60	1	188.1
15	65	1	209.
15	70	1	229.9
15	75	1	250.8
15	80	1	271.7
15	85	1	292.6
15	90	1	313.5

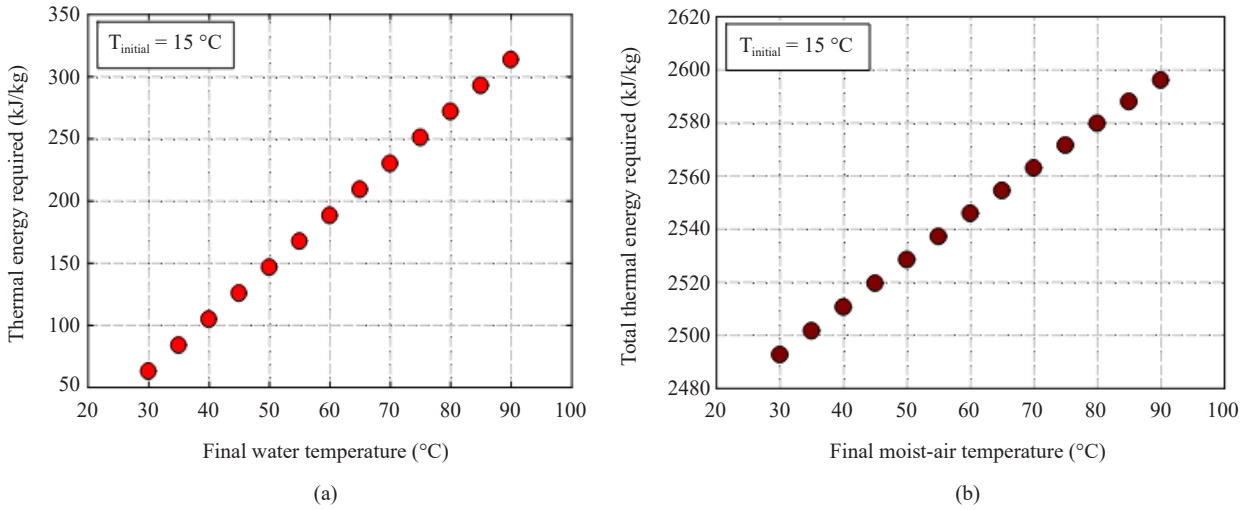

Figure 6. (a) Heat energy necessary for the water in the tank. (b) The latest heat energy necessary for the moist air

As adiabatically saturated moist air traverses a chill environment, its energy content diminishes due to heat transfer. The magnitude of this energy transfer can be assessed by analysing the enthalpy change of the working air, which depends on the first and latest state temperatures. Utilising the psychometric diagram facilitates the straightforward visualisation of enthalpy change. The enthalpy variation for various temperature values of warm, humid air in the first state is outlined in Table 2. This table serves as a valuable reference for understanding the alterations in energy content under different temperature conditions.

Table 2. Under various first conditions enthalpy exchange of air

First water temperature (°C)	Relative humidity (%)	First enthalpy (kJ/kg)	Latest enthalpy (kJ/kg)	Enthalpy change (kJ/kg)
30	100	99.7	76.30	23.4
35	100	129	76.30	52.7
40	100	166	76.30	89.7
45	100	213.2	76.30	136.9
50	100	274	76.30	197.7
55	100	353.2	76.30	276.9
60	100	458.1	76.30	381.8
65	100	599.9	76.30	523.6
70	100	797.4	76.30	721.1
75	100	1,084.2	76.30	1,007.9
80	100	1,527.4	76.30	1,451.1
85	100	2,283.7	76.30	2,207.4
90	100	3,823.4	76.30	3,747.1

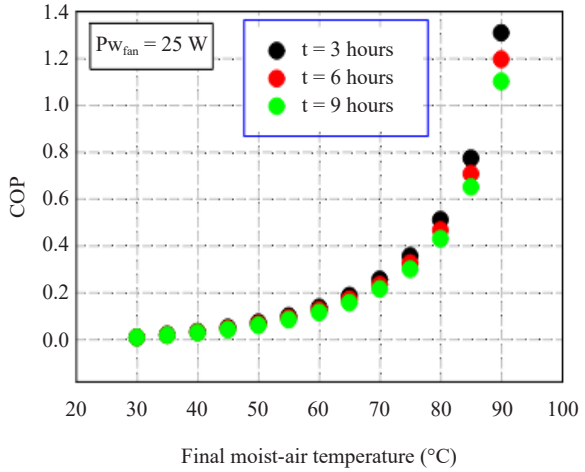
Pw$_{fan}$ = 25 W
t = 3 hours
t = 6 hours
t = 9 hours
COP
Final moist-air temperature (°C)

(a)

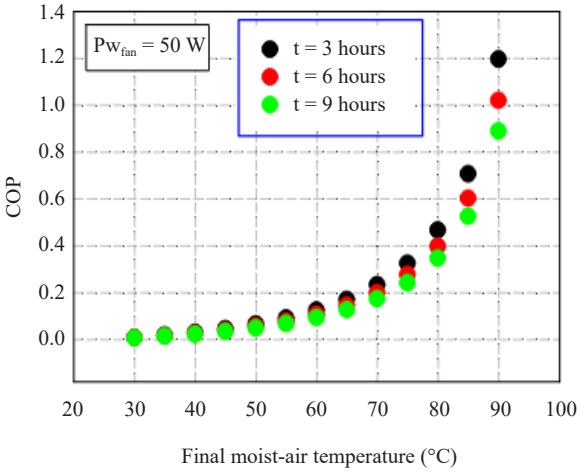
Pw$_{fan}$ = 50 W
t = 3 hours
t = 6 hours
t = 9 hours
COP
Final moist-air temperature (°C)

(b)

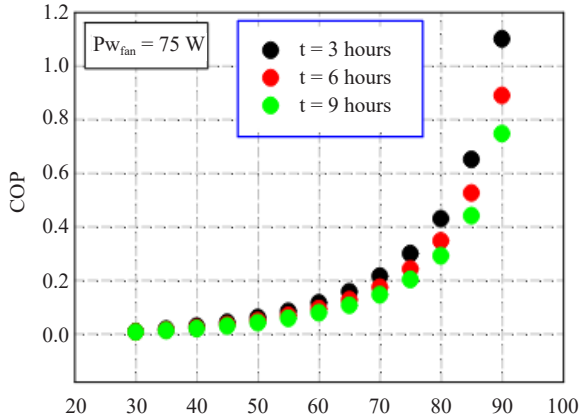
Pw$_{fan}$ = 75 W
t = 3 hours
t = 6 hours
t = 9 hours
COP
Final moist-air temperature (°C)

(c)

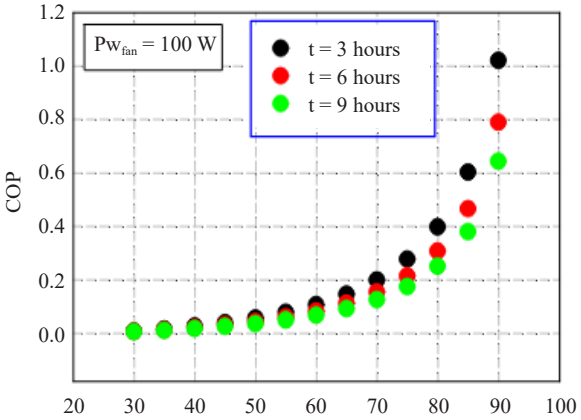
Pw$_{fan}$ = 100 W
t = 3 hours
t = 6 hours
t = 9 hours
COP
Final moist-air temperature (°C)

(d)

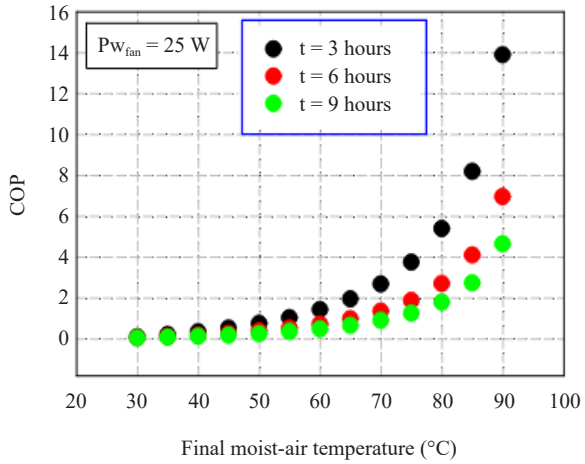
Pw$_{fan}$ = 25 W
t = 3 hours
t = 6 hours
t = 9 hours
COP
Final moist-air temperature (°C)

(e)

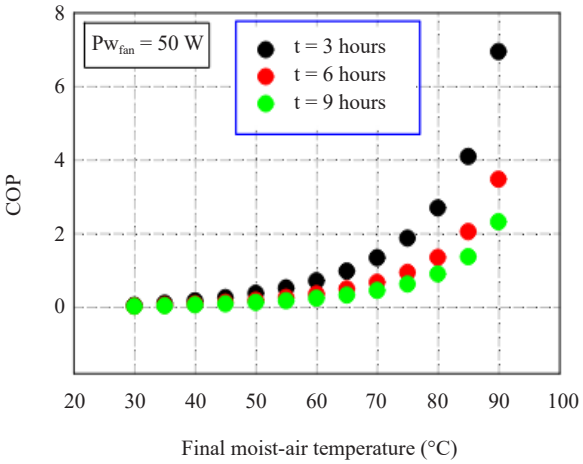
Pw$_{fan}$ = 50 W
t = 3 hours
t = 6 hours
t = 9 hours
COP
Final moist-air temperature (°C)

(f)

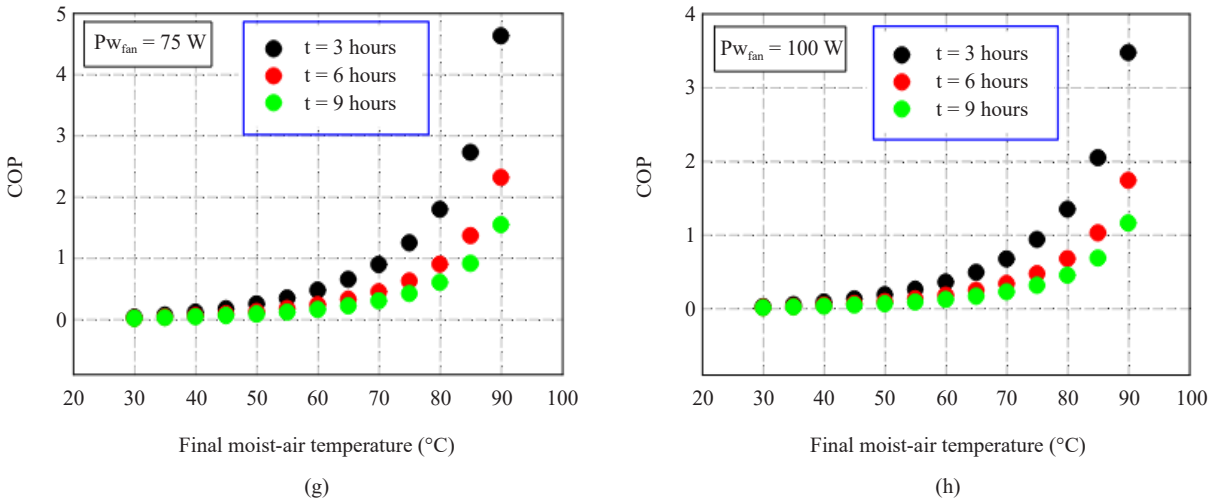

Figure 7. COP values for different operation times of MAS with a fan power of (a) 25 W, (b) 50 W, (c) 75 W, (d) 100 W. COP values for different operation times of MAS with a fan power (e) 25 W, (f) 50 W, (g) 75 W, (h) 100 W fed by solar energy

The thermal performance of MAS exhibits variability across different fan power and operating process values. Fan power ranges from 25 to 100 W, whilst operating time varies from 3 to 9 hours per day. These specified operational parameters are designed to encompass a broad spectrum of climatic conditions. Apart from the unattached parameters, the latest water temperature is in addition to examined as a significant parameter influencing the COP of MAS. This comprehensive analysis allows for a nuanced understanding of MAS performance under diverse conditions.

Table 3. COP values for different operation times of MAS with a fan power of 25 W, 50 W, 75 W, and 100 W

	Final moist-air temperature (°C)			COP		
			25 W			
	9 hours	6 hours	3 hours	9 hours	6 hours	3 hours
Min.	30	30	30	0.00777778	0.00777778	0.00777778
Max.	90	90	90	1.10444	1.20556	1.31444
			50 W			
Min.	30	30	30	0.0157303	0.0157303	0.0157303
Max.	90	90	90	0.888764	1.04247	1.20337
			75 W			
Min.	30	30	30	0.0205714	0.0205714	0.0205714
Max.	90	90	90	0.761143	0.898286	1.11086
			100 W			
Min.	30	30	30	0.00685714	0.00685714	0.00685714
Max.	90	90	90	0.644571	0.795429	1.02171

The analyses are conducted in two scenarios: with and without renewable energy production. Under the situation of renewable energy production, the MAS is accepted to be utilised with solar collectors and PV panels. Conversely, in the absence of renewable energy production, it is putative that the energy required by MAS will be solely sourced from electrical energy. The analyses conducted for each separate situation are illustrated in Figure 7, providing insights into the system's performance under different energy sourcing scenarios. The impacts of utilising electricity and solar energy on the COP are illustrated in Tables 3 and 4.

Table 4. COP values for different operation times of MAS with a fan power 25 W, 50 W, 75 W, and 100 W fed by solar energy

	Final moist-air temperature (°C)			COP		
			25 W			
	9 hours	6 hours	3 hours	9 hours	6 hours	3 hours
Min.	30	30	30	0.0888889	0.0888889	0.0888889
Max.	90	90	90	4.62222	4.08889	8.17778
			50 W			
Min.	30	30	30	0.0415706	0.0487805	0.0487805
Max.	90	90	90	2.4878	3.5122	6.92683
			75 W			
Min.	30	30	30	0.0584795	0.0584795	0.0584795
Max.	90	90	90	1.57895	2.30994	0.0584795
			100 W			
Min.	30	30	30	0.0243902	0.0731707	0.0243902
Max.	90	90	90	1.19512	1.78049	3.43902

Tables 3 and 4 present a comprehensive analysis delineating the hourly Coefficient of Performance (COP) values within the context of this innovative system, contingent upon varying sources of energy provision. Through a meticulous examination of these tables, one can discern the dynamic interplay between the system's efficiency and the diverse energy inputs it accommodates.

6.2 *Heat transfer analysis of moist airflow system*

This section encompasses a comprehensive heat transfer analysis aimed at determining the optimal channel dimensions for various channel lengths and operating times. The analysis considers the length of the canal ranging from 40 to 70 m, with working times of 1, 1.5, and 2 h as unattached parameters. To deepen comprehension, the diameter of the duct for each state is calculated, and the results are explicated. The analysis reveals that the diameter of the duct significantly correlates with both the latest moist air temperature and the length of channel, as displayed in Figure 8. Consequently, there is a recognisable increase in the channel diameter as the moist air temperature rises in each scenario. It is anticipated that the heat transfer phenomenon necessitates smaller channel diameter with increasing operating times.

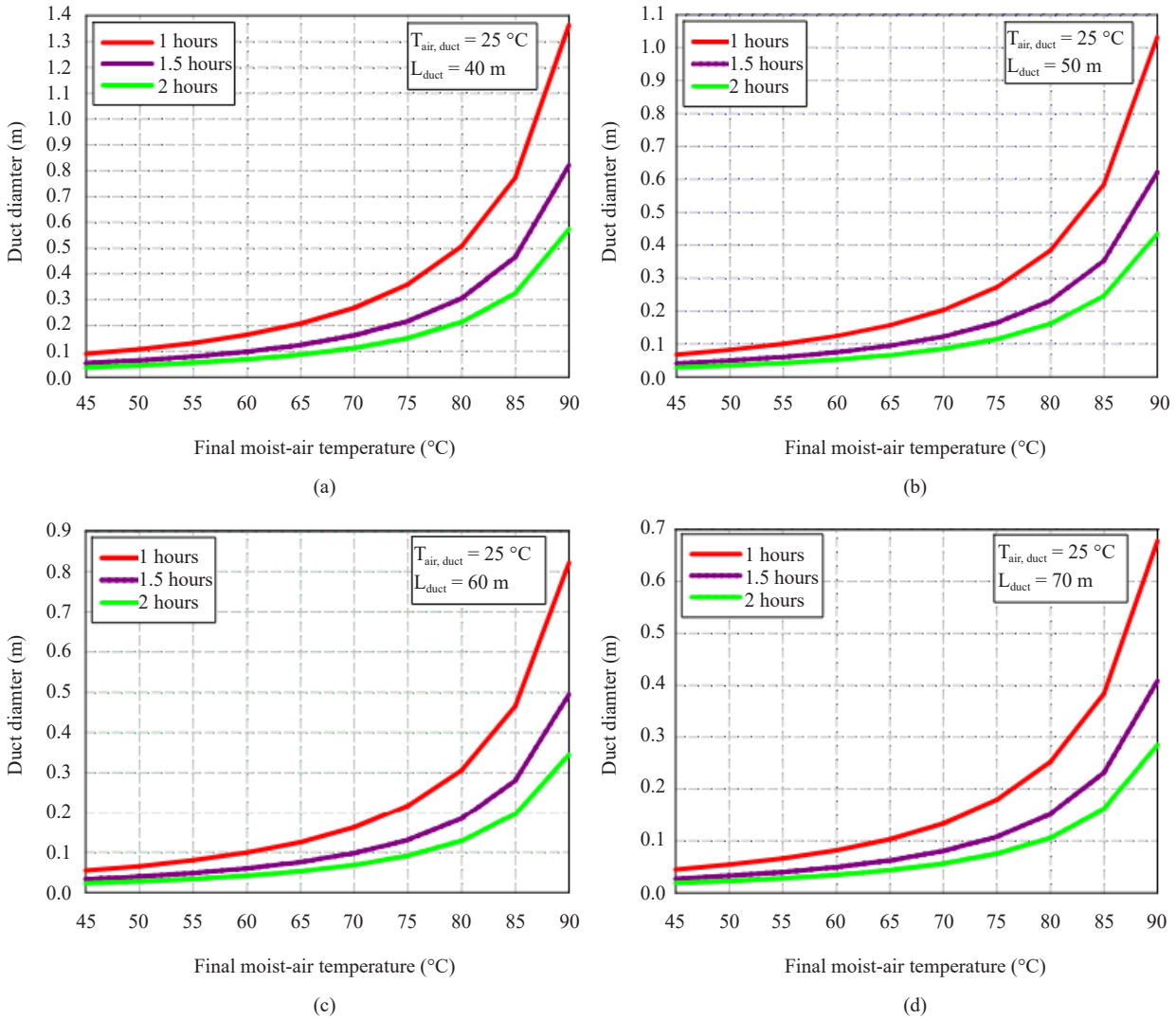

Figure 8. The relationship between diameter of the duct and operation time across four different length of ducts for (a) 40 m, (b) 50 m, (c) 60 m, and (d) 70 m

Figure 9 illustrates how length of the duct affects diameter of the channel across different heat output values. The linear relationship between diameter of the duct and heat output is observed in all examined scenarios. It is observed that the diameter of the duct shows a consistent upward trend as the heat output increases across various operation times. The figures also depict a slight decrease in diameter of the duct with increased operation time. Overall, it's apparent that the temperature of latest moist air, length of duct, operation time, and heat output are key parameters influencing diameter of the duct assignment in specific cases. Optimisation of these independent variables is essential for accurate and reliable estimation of diameter of the duct within the system.

6.3 *Duct diameter analysis of moist airflow system*

Figure 10 displays the rate of diameter of the duct for both heating systems of water-based and air-based in relation to the temperature difference of the drive fluid, analysed within the 50-75 °C range. The results represent a rising trend in the diameter of the duct with increasing temperature differences of the drive fluid. This trend stems from the more significant variation in diameter of the duct observed in water-based systems compared to air-based systems due to temperature differences. Additionally, the data demonstrate that the diameter of the duct of water-based systems is

considerably smaller compared to that of air-based systems, indicating inherent distinctions in density values between the two mediums.

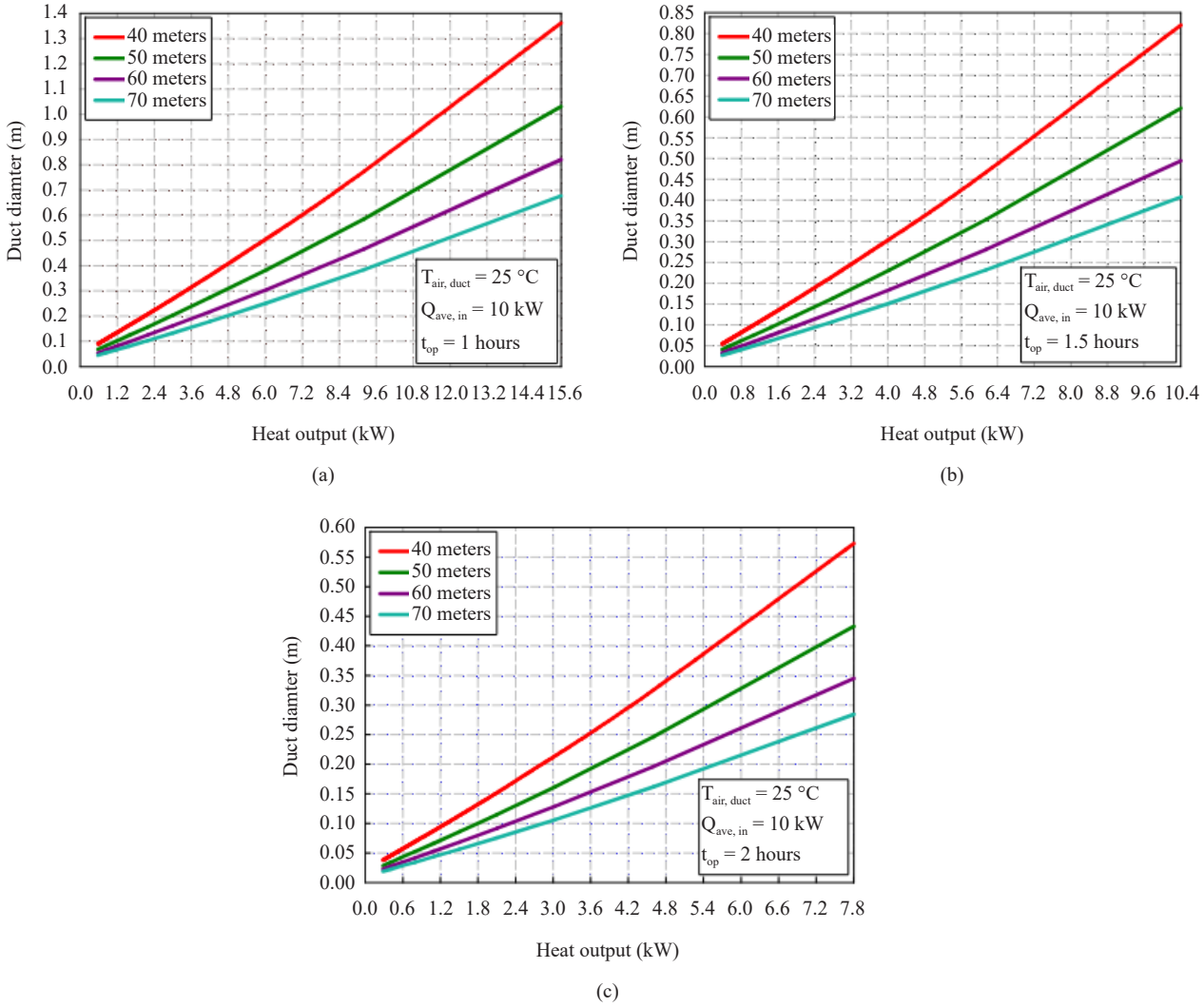

Figure 9. The relationship between diameter of the duct, heat output, and length of duct from 40 to 70 meters across three different operation times for (a) 1 h, (b) 1.5 h, and (c) 2 h

Figure 11 (a) represents the relationship between the diameter of the duct rate of heating systems of water and moist air-based and the temperature difference. The findings reveal a consistent pattern; however, the diameter of the duct values suggest that the heating system of moist air-based possesses a smaller diameter of the duct compared to the dry-air system operating at the same temperature. For easier interpretation of the results, Figure 11 (b) showcases the fluctuation of diameter of the duct concerning the temperature difference of the drive fluid. Analysis of the data suggests that the heating system of air-based achieves the greatest diameter of the duct, while the system employing water as the drive fluid achieves the lowest. This outcome aligns with expectations and can be attributed to variations in density and specific heat capacity across the systems.

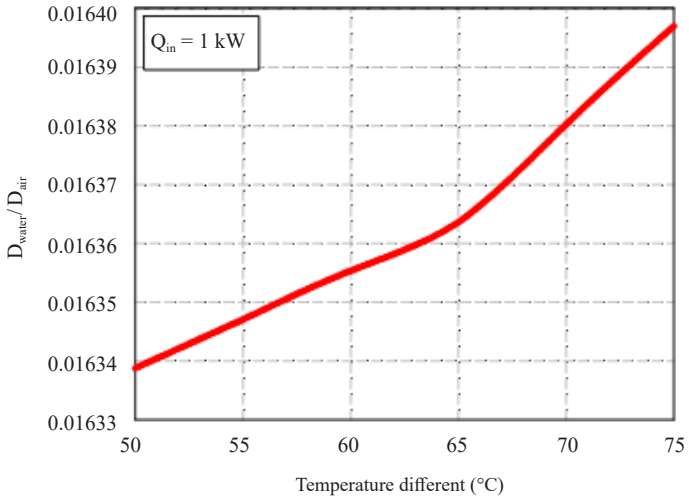

Figure 10. The diameter of the duct rate between water and air-based heating systems

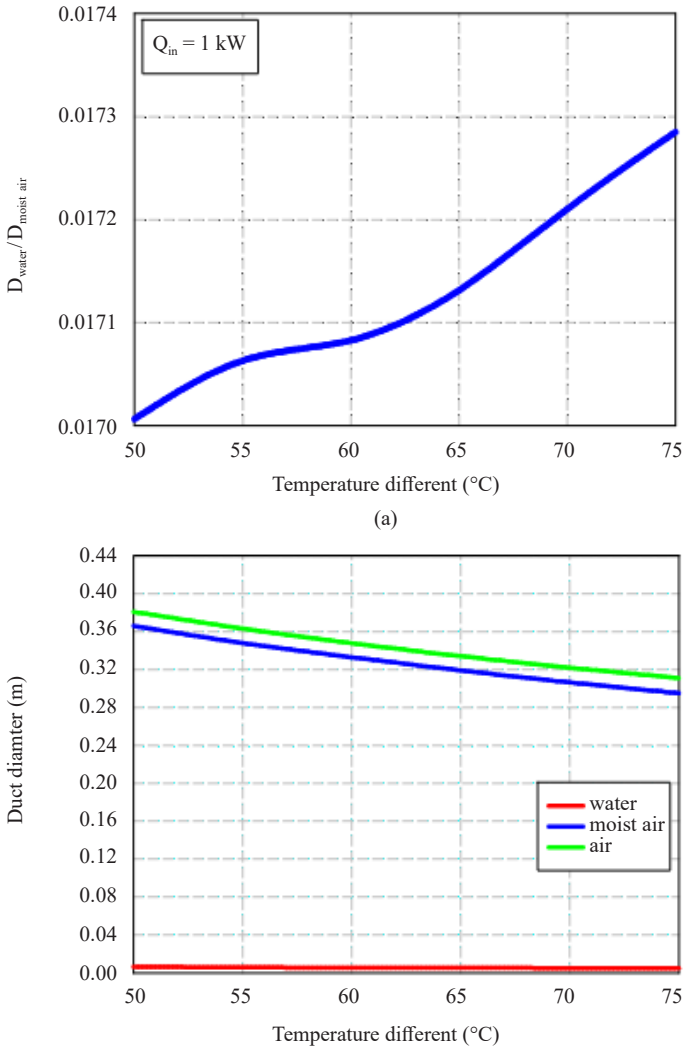

Figure 11. (a) Diameter of the duct rate of water and heating system of moist air-based, (b) Diameter of the duct comparison for water, moist air and air

7. Conclusion

Buildings contribute significantly to global energy consumption, highlighting the urgency of cost-effective solutions to lessen their energy utilisation. The prevalent lack of efficient thermal insulation in traditional building materials results in substantial heating demands across the current global building inventory. Consequently, extensive endeavours are underway to curtail heating requirements through affordable and eco-friendly initiatives. Nevertheless, scientists widely agree that additional advancements are indispensable to fulfil the latest low-carbon objectives set forth by developed nations. This study introduces a novel heating system termed the MAS and investigates its thermal performance under various operational parameters. Employing a thermodynamic-based modelling approximation coupled with comprehensive heat transfer analysis, the research yields the following conclusive results:

• The thermal performance of the MAS is significantly have affect by the temperature of the moist air, the power of the fan, and the duration of the operation.

• The COP values exhibit great promise, particularly in configurations involving a solar thermal collector and PV panel. These values span a range from 0.007 to 13.878, contingent upon factors such as moist air temperature, fan power, and operational duration.

• Without incorporating renewable energy generation or waste heat recovery mechanisms, the maximum achievable COP is approximately 1.307.

• With a constant value of the length of the duct, there is a slight decrease in the diameter of the duct as the operation time increases.

• As the length of the duct increases, a slight decrease is observed in its diameter.

• As the latest moist air temperature increases, there is an exponential growth in the diameter of the duct.

• The diameter of the duct increases in a linear fashion, correlating with the rising trend of the system's heat output.

• In a specific instance characterised by a moist air output temperature of 25 °C, a 10 kW heat input, a 2-hour operation time, and a 6 kW heat output, the diameter of the duct varies. For the lengths of ducts of 70, 60, 50, and 40 meters, the respective diameter of the ducts is measured at 22, 26, 32, and 43 centimetres.

• The effectiveness of the MAS in alleviating building heating demands becomes highly appealing, provided it can be sustained by renewable energy sources and if the climatic conditions remain moderate.

This research encompasses an analysis of the diameter of the duct for a novel heating system across three distinct drive fluids: air, moist air, and water. The study involves a flat power input (1 kW) to the reference system and is performed over a temperature difference range of 50-75 °C.

• The findings suggest that the diameter of the duct of a system of water-based is notably smaller compared to that of an air-based system, influenced by differences in density values. This trend is similarly observed in the diameter of the duct ratio of heating system of water and moist air based.

• The heating system of air-based demands the largest diameter of the duct for the same temperature difference, while the water-based system requires the smallest. This contrast arises due to differences in density and specific heat capacity among the systems.

• In further works, PV cell parameters can be related to the environmental and operating conditions for a complete thermodynamic performance assessment [33, 34] in energy generation part of the system.

• The MAS has a considerable potential for meeting the low/zero carbon targets released for 2030 and 2050 buildings [35].

The cost-effectiveness of the MAS surpasses that of conventional heating systems, given its reliance solely on a fan and utilisation of moist air as the drive fluid. This innovative system holds the potential to significantly reduce greenhouse gas emissions originating from buildings.

Conflict of interest

There is no conflict of interest among the authors.

References

[1] González-Torres M, Pérez-Lombard L, Coronel JF, Maestre IR, Yan D. A review on buildings energy information: Trends, end-uses, fuels and drivers. *Energy Reports*. 2022; 8: 626-637.

[2] Wang Z, Yang Z, Zhang B, Li H, He W. How does urbanisation affect energy consumption for central heating: Historical analysis and future prospects. *Energy and Buildings*. 2022; 255: 111631.

[3] Maduru VR, Shaik S, Cuce E, Afzal A, Panchal H, Cuce PM. UV coated acrylics as a substitute for generic glazing in buildings of Indian climatic conditions: Prospective for energy savings, CO_2 abatement, and visual acceptability. *Energy and Buildings*. 2022; 268: 112231.

[4] Cuce PM, Cuce E, Alvur E. Internal or external thermal superinsulation towards low/zero carbon buildings? A critical report. *Gazi Mühendislik Bilimleri Dergisi*. 2024; 9(3): 435-442.

[5] Al Dakheel J, Del Pero C, Aste N, Leonforte F. Smart buildings features and key performance indicators: A review. *Sustainable Cities and Society*. 2020; 61: 102328.

[6] Besir AB, Cuce E. Green roofs and facades: A comprehensive review. *Renewable and Sustainable Energy Reviews*. 2018; 82: 915-939.

[7] Yang X, Hu M, Heeren N, Zhang C, Verhagen T, Tukker A, et al. A combined GIS-archetype approach to model residential space heating energy: A case study for the Netherlands including validation. *Applied Energy*. 2020; 280: 115953.

[8] Cuce E, Cuce PM, Wood C, Gillott M, Riffat S. Experimental investigation of internal aerogel insulation towards low/zero carbon buildings: A comprehensive thermal analysis for a UK building. *Sustainable and Clean Buildings*. 2024; 1(1): 1-22.

[9] Economidou M, Todeschi V, Bertoldi P, D'Agostino D, Zangheri P, Castellazzi L. Review of 50 years of EU energy efficiency policies for buildings. *Energy and Buildings*. 2020; 225: 110322.

[10] Balali Y, Chong A, Busch A, O'Keefe S. Energy modelling and control of building heating and cooling systems with data-driven and hybrid models-A review. *Renewable and Sustainable Energy Reviews*. 2023; 183: 113496.

[11] Hamidinasab B, Javadikia H, Hosseini-Fashami F, Kouchaki-Penchah H, Nabavi-Pelesaraei A. Illuminating sustainability: a comprehensive review of the environmental life cycle and exergetic impacts of solar systems on the agri-food sector. *Solar Energy*. 2023; 262: 111830.

[12] Vaishnav P, Fatimah AM. The environmental consequences of electrifying space heating. *Environmental Science & Technology*. 2020; 54(16): 9814-9823.

[13] Wang Y, Wang J, He W. Development of efficient, flexible and affordable heat pumps for supporting heat and power decarbonisation in the UK and beyond: Review and perspectives. *Renewable and Sustainable Energy Reviews*. 2022; 154: 111747.

[14] Scheffran J, Felkers M, Froese R. Economic growth and the global energy demand. In *Green Energy to Sustainability: Strategies for Global Industries*. NJ: John Wiley & Sons Ltd.; 2020. p.1-44.

[15] Santamouris M, Vasilakopoulou K. Present and future energy consumption of buildings: Challenges and opportunities towards decarbonisation. *e-Prime-Advances in Electrical Engineering, Electronics and Energy*. 2021; 1: 100002.

[16] Cabeza LF, Chàfer M. Technological options and strategies towards zero energy buildings contributing to climate change mitigation: A systematic review. *Energy and Buildings*. 2020; 219: 110009.

[17] Akram MW, Hasannuzaman M, Cuce E, Cuce PM. Global technological advancement and challenges of glazed window, facade system and vertical greenery-based energy savings in buildings: A comprehensive review. *Energy and Built Environment*. 2023; 4(2): 206-226.

[18] Rashid FL, Al-Obaidi MA, Dulaimi A, Mahmood DM, Sopian K. A review of recent improvements, developments, and effects of using phase-change materials in buildings to store heat energy. *Designs*. 2023; 7(4): 90.

[19] Verbeke S, Audenaert A. Thermal inertia in buildings: A review of impacts across climate and building use. *Renewable and Sustainable Energy Reviews*. 2018; 82: 2300-2318.

[20] Cuce E, Cuce PM, Alvur E, Yilmaz YN, Saboor S, Ustabas I, et al. Experimental performance assessment of a novel insulation plaster as an energy-efficient retrofit solution for external walls: A key building material towards low/zero carbon buildings. *Case Studies in Thermal Engineering*. 2023; 49: 103350.

[21] Saxena A, Cuce E, Kabeel AE, Abdelgaied M, Goel V. A thermodynamic review on solar stills. *Solar Energy*. 2022; 237: 377-413.

[22] Cuce E, Cuce PM, Saxena A, Guclu T, Besir AB. Performance analysis of a novel solar desalination system-Part 1: The unit with sensible energy storage and booster reflector without thermal insulation and cooling system.

Sustainable Energy Technologies and Assessments. 2020; 37: 100566.
[23] Aditya GR, Mikhaylova O, Narsilio GA, Johnston IW. Comparative costs of ground source heat pump systems against other forms of heating and cooling for different climatic conditions. *Sustainable Energy Technologies and Assessments*. 2020; 42: 100824.
[24] Bahrami M, Pourfayaz F, Kasaeian A. Low global warming potential (GWP) drive fluids for Organic Rankine Cycle (ORC) applications. *Energy Reports*. 2020; 8: 2976-2988.
[25] Mohammadi O, Shafii MB, Rezaee Shirin-Abadi A, Heydarian R, Ahmadi MH. The impacts of utilizing nano-encapsulated PCM along with RGO nanosheets in a pulsating heat pipe, a comparative study. *International Journal of Energy Research*. 2021; 45(13): 19481-19499.
[26] Assareh E, Ghafouri A. An innovative compressed air energy storage (CAES) using hydrogen energy integrated with geothermal and solar energy technologies: A comprehensive techno-economic analysis-different climate areas-using artificial intelligent (AI). *International Journal of Hydrogen Energy*. 2023; 48(34): 12600-12621.
[27] Di Rocco AR, Bottino-Leone D, Troi A, Herrera-Avellanosa D. Application of the guidelines for the integration of photovoltaics in historic buildings and landscapes to evaluate the best practices of the historic building energy retrofit atlas. *Buildings*. 2024; 14(2): 499.
[28] Ni HP, Chong WO, Chou JS. Optimizing HVAC systems for semiconductor fabrication: a data-intensive framework for energy efficiency and sustainability. *Journal of Building Engineering*. 2024; 89: 109397.
[29] Jacobs S, van Minnebruggen S, Matbouli H, Ghane S, Hellinckx P, Verhaert I. Evaluating innovative collective heating and cooling concepts by incorporating occupants' preferences for conflicting performance indicators. *Energy and Buildings*. 2024; 314: 114264.
[30] Hassanpour H, Hamedi AH, Mhaskar P, House JM, Salsbury TI. A hybrid clustering approach integrating first-principles knowledge with data for fault detection in HVAC systems. *Computers & Chemical Engineering*. 2024; 187: 108717.
[31] Cuce E, Cuce PM, Sen H. A thorough performance assessment of solar chimney power plants: Case study for Manzanares. *Cleaner Engineering and Technology*. 2020; 1: 100026.
[32] Salama A. Velocity profile representation for fully developed turbulent flows in pipes: a modified power law. *Fluids*. 2021; 6(10): 369.
[33] Cuce E, Bali T. Variation of cell parameters of a p-Si PV cell with different solar irradiances and cell temperatures in humid climates. In *Fourth International Exergy, Energy and Environment Symposium*. Sharjah, United Arab Emirates; 2009.
[34] Cuce E. *Thermodynamic Analysis of the Effectiveness of Different Types of PV Modules for Wet Conditions*. M.Sc. Thesis. Karadeniz Technical University. 2009.
[35] Cuce E. *Development of Innovative Window and Fabric Technologies for Low-Carbon Buildings*. Ph.D. Thesis. The University of Nottingham. 2014.